

# Smallest possible electromagnetic mode volume in a dielectric cavity

R. Coccioli  
M. Boroditsky  
K.W. Kim  
Y. Rahmat-Samii  
E. Yablonovitch

Indexing terms: Mode volume, Electromagnetic waves, Photonic crystals, Spontaneous emission, Purcell effect

**Abstract:** In photonic crystals, electromagnetic waves can be confined in all three dimensions – leading to very small mode volumes. A computational search has been made for the smallest electromagnetic mode volume which occurs in two-dimensional, dielectric photonic crystals slabs. The smallest mode volume found was  $V \approx 2(\lambda/2n)^3$ , where  $n$  is the refractive index. This small mode volume can lead to significant enhancement of spontaneous emission rates in semiconductor nano-cavities due to the Purcell effect.

## 1 Introduction

The spontaneous emission rate of an atom can be increased or decreased by changing its environment. Photonic crystals (artificially created, multidimensionally periodic structures) are known to exhibit a forbidden bandgap for electromagnetic wave propagation, and thus, can be used to modify spontaneous emission. Initially, it was proposed to use photonic crystals to inhibit spontaneous emission [1], but they can also be employed to enhance it.

It has been known since 1946 that enhancement of the spontaneous emission rate (the Purcell effect) can be achieved in very tiny electromagnetic cavities [2]. It is tempting to apply the Purcell effect to the spontaneous emission of optoelectronic materials [3], such as III–IV semiconductors. Several examples have recently appeared: a five-fold increase in the radiative rate was demonstrated at low temperatures in VCSEL-type micro-cavities by Gerard *et al.* [4]. Likewise, layered one-dimensional Bragg micro-cavities increase the efficiency of planar light emitting diodes (LEDs), as proposed by Schubert *et al.* [5] and most successfully realised by De Neve *et al.* [6].

It can be shown (see Appendix) that the enhancement of spontaneous emission rate in a semiconductor nano-cavity structure with a quantum well active region is

$$\frac{\Gamma}{\Gamma_0} = \frac{3Qg(\lambda/2n)^3}{2\pi V_{eff}} \quad (1)$$

where  $Q$  is the quality factor of the cavity,  $n$  is the refractive index of the semiconductor,  $\lambda$  is the mode's wavelength,  $g$  is the mode degeneracy factor, and  $V_{eff}$  is the mode volume, defined as

$$V_{eff} = \frac{\int \varepsilon(\mathbf{r}) \mathbf{E}^2(\mathbf{r}) d^3\mathbf{r}}{(\varepsilon(\mathbf{r}) \mathbf{E}^2(\mathbf{r}))_{max}} \quad (2)$$

The integration in eqn. 2 is performed over the quantisation volume, as described in the Appendix. It is possible to build a very high  $Q$  dielectric cavity using photonic crystals, but once the spectral width  $\Delta\nu = \nu/Q$  of a resonant cavity is smaller than the line width  $\Delta\nu_m$  of the spontaneous emission, there is no further increase in the spectrally integrated spontaneous emission rate. The normal spontaneous emission bandwidth of optoelectronic semiconductors at room temperature limits the useable cavity to  $Q > 10$  or  $Q > 40$ , depending on the specific material. Looking at eqn. 2, significant enhancement of spontaneous emission rate in semiconductors at room temperature requires building the smallest possible electromagnetic cavities or, in other words, reducing the effective volume  $V_{eff}$ . This makes the search for the smallest mode volume achievable with the dielectric material an important requirement. The value  $V_{eff} = 2.55(\lambda/2n)^3$  has previously been reported by Foresi *et al.* [7], [Note 1] for a one-dimensional bridge photonic crystal. Is it possible to do better?

The minimal size of a dielectric cavity mode is the focus of this paper. We have used the finite difference time domain (FDTD) method to compute the smallest achievable effective volume. The FDTD method has been chosen because of its capability to deal with complicated structures such as those analysed here. Using different kinds of boundary conditions, the method allows us to deal with many different types of problem: computation of dispersion diagram, and computation of resonant frequency, effective mode volume,  $Q$ , and mode pattern in the nano-cavity. FDTD was used by Sakoda [8] to study modal properties of defects in infinite 2-D photonic crystals without considering mode volume. Indeed, the method proved to be very effective in this calculation because it provides a wealth of data, from which it is possible to derive all the quantities of

Note 1: The mode volume given in [7] is twice as large due to a different definition. We chose the definition in Eqn. 2 as it agrees with the implicit definition given in Purcell, ref. 2

© IEE, 1998

IEE Proceedings online no. 19982468

Paper received 19th May 1998

The authors are with the Electrical Engineering Department, University of California, Los Angeles, 405 Hilgard Avenue, Los Angeles, CA 90095 USA

interest for the design of nano-cavities. The code implemented has been extensively tested against data available in the literature. Using this valuable numerical tool, we show that an effective volume  $V_{eff} \approx 2(\lambda/2n)^3$  is achievable. As a complementary result, Painter *et al.* have demonstrated that very high  $Q \approx 4000$  can be achieved in similar thin-slab PBG cavities at the price of a slightly greater mode volume.

We have analysed numerous possible configurations of dielectric cavity created by the introduction of a defect into a two-dimensional photonic crystal. Our base-line 2-D photonic crystal consisted of a thin slab with a triangular array of holes. Our choice of such a structure in Fig. 1a is justified by the following considerations: this type of 2-D photonic crystal structure shows a large bandgap for TE polarisation, providing good horizontal confinement. Guided modes in such a structure are vertically well confined by the slab refractive index, and so the vertical dimension of the mode is small. Finally, this structure is much easier to fabricate at the optical wavelength scale than three-dimensional photonic crystals. We have considered only donor modes, i.e. modes created by adding some extra material to the photonic crystal. In such donor mode cavities, the electromagnetic field tends to be concentrated in the regions where dielectric material has been added. For spontaneous emission there has to be a good overlap between the electromagnetic field and the semiconductor light emitter. In all our computations, we considered a thin semiconductor slab with refractive index 3.5 bonded to a glass substrate with refractive index 1.5.

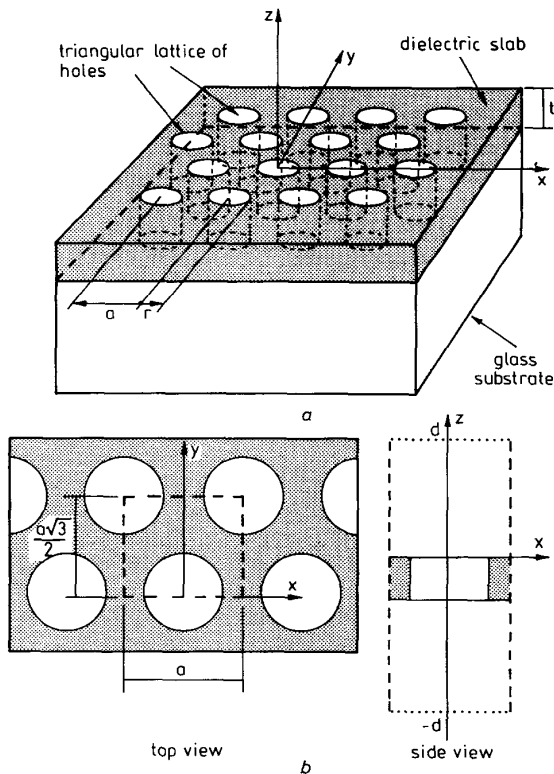


**Fig. 1** Baseline configuration  
 a Small section of infinite dielectric slab with triangular array of through holes resting on a glass substrate; b Unit cell used for the computation of the frequency  $\nu$  against wavevector  $\mathbf{k}$  dispersion relationship of the infinite photonic crystal corresponding to a  
 ..... absorbing boundary conditions  
 - - - - - periodic Bloch boundary conditions

## 2 Numerical results: dispersion diagram

Computation of the dispersion diagram of the photonic crystal shown in Fig. 1a implies considering propagation of the electromagnetic wave in the infinite space tiled with identical cells in the  $xy$ -plane. The solution of Maxwell's equations must satisfy Bloch periodic conditions:

$$\mathbf{E}(\mathbf{r} + \mathbf{a}, t) = \mathbf{E}(\mathbf{r}, t)e^{i\mathbf{k} \cdot \mathbf{a}} \quad \mathbf{H}(\mathbf{r} + \mathbf{a}, t) = \mathbf{H}(\mathbf{r}, t)e^{i\mathbf{k} \cdot \mathbf{a}} \quad (3)$$

with  $\mathbf{a}$  is a primitive lattice vector, and  $\mathbf{k}$  is the wave vector.

At any instant of time, the phase shift  $e^{i\mathbf{k} \cdot \mathbf{a}}$  is the only difference between the eigenmode's fields at corresponding points in different cells. Consequently, the computational domain for the analysis may be restricted to a single unit cell of the crystal, delimited by the constant co-ordinate surfaces  $x = \pm a/2$ ,  $y = 0$ , and  $y = a\sqrt{3}/2$  (Fig. 1b). At those surfaces, the periodic Bloch boundary conditions (eqn. 3) must be applied to the tangential component of the electric and magnetic fields, where now the lattice vector  $\mathbf{a}$  connects corresponding points at the opposite sides of the unit cell. The thin dielectric film with a triangular lattice of holes (Fig. 1a) does not possess periodicity in the vertical direction. For that reason the computational domain shown in Fig. 1b is terminated using absorbing boundary conditions (ABC) at the surfaces  $z = \pm d$ . Both Mur's first-order boundary conditions [9] and anisotropic perfectly matched layer absorbing boundary conditions [10, 11] (PML) have been used in our work.

The structure can be excited either with some initial electromagnetic field distribution or with one or more arbitrarily oriented dipoles, using a Gaussian pulse in time. If a localised source is used to excite the structure, its spectrum must be wide enough to cover the frequency range of interest. The FDTD marching-in-time scheme is applied to compute the electromagnetic field in the computational domain. Owing to the Bloch periodic boundary conditions (eqn. 3), the electromagnetic field will reach a steady state after all radiative modes are absorbed by the ABCs. For each value of the wave vector  $\mathbf{k}$ , Maxwell's equations are solved and the field is observed at certain points in the unit cell. These are chosen away from the symmetry planes of the lattice, unless some particular symmetry class of the modes is under consideration, to avoid the possibility of probing the field in the node of a possible mode.

The Fourier transform of the computed signal has peaks at frequencies of the vertically confined modes that can propagate in the structure with the given wave vector  $\mathbf{k}$ . The computational time must be long enough to allow the desired frequency resolution.

We have computed the dispersion diagram  $\nu$  against  $k$  of the perforated dielectric slab ( $\epsilon = 12$ ) sitting on a glass substrate ( $\epsilon = 2.25$ ) (Fig. 1a) using this technique. Wave propagation in a similar freestanding structure was previously calculated using the plane wave expansion method with the super-cell approach [12]. Fig. 2 shows the dispersion diagram for the TE-like guided modes of the structure when the propagation vector  $\mathbf{k}$  lies in the  $x$ - $y$  plane. The ratio between the thickness  $t$  of the slab and the lattice constant  $a$  was chosen to be  $t/a = 0.333$ , and the radius  $r$  of the holes was chosen to be  $r = 0.40 a$ . These parameters seem to give the smallest possible mode volume. A wide forbidden gap for

the TE-like modes exists in the range of normalised frequencies  $0.33 c/a \leq \nu \leq 0.43 c/a$ . As shown below, this two-dimensional photonic band structure can be used as a reflecting medium to create a cavity with a very small mode volume.

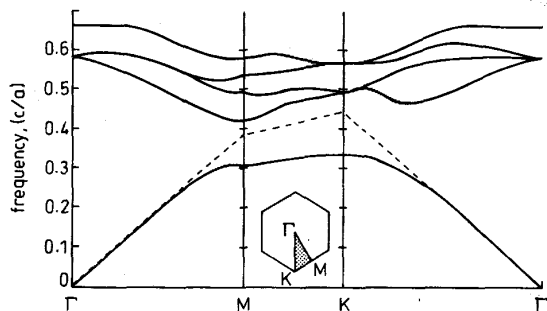


**Fig. 2** Dispersion diagram of TE-like modes of the infinite photonic crystal shown in Fig. 1a  
To set the horizontal scale,  $\Gamma M = 2\pi\sqrt{3}a$   
--- upper limit to the modes which are confined to the slab and cannot leak into the glass substrate

### 3 Numerical results: investigation of candidate nano-cavities

Introduction of an irregularity in the periodic structure of a photonic crystal, often referred to as a defect, may cause localisation of one or more electromagnetic modes around the defect itself. To completely characterise these localised resonant modes, we have considered a finite sized photonic crystal with a defect close to its centre, and we have employed the FDTD using absorbing boundary conditions on all boundaries of the computational domain.

The Fourier transform of the electromagnetic field at observation points inside the cavity gives the resonant frequencies of the cavity, and the  $Q$  of each mode can be estimated from the decay rate of the energy stored in the cavity. Note that the numerical computation of cavity  $Q$  is very sensitive to several parameters: in particular, to the value of the dielectric material, to the kind of absorbing boundary conditions used to terminate the computational domain, and to the distance between the open dielectric cavity and the boundary of the computational domain.

As mentioned above, to achieve high enhancement of spontaneous emission rate the resonant mode of a cavity must have the smallest possible volume while its  $Q$  must be greater than  $Q_m = \nu_m/\Delta\nu_m$  of the active material [13], where  $\nu_m$  and  $\Delta\nu_m$  are the frequency and line width of the material transition, respectively. A figure-of-merit for cavity optimisation is the mode's effective volume normalised to the cubic half wavelength of the resonant mode  $(\lambda/2n)^3$  in the medium of refractive index  $n$ :

$$\frac{V_{eff}}{(\lambda/2n)^3} = \frac{\int \epsilon(\mathbf{r})\mathbf{E}^2(\mathbf{r})d^3\mathbf{r}}{(\lambda/2n)^3 (\epsilon(\mathbf{r})\mathbf{E}^2(\mathbf{r}))_{max}} \quad (4)$$

The FDTD algorithm allows computation of the effective volume either in the time domain or in the frequency domain by postprocessing the computed data. Particular care must be exercised to deal with some numerical issues when computing the effective mode volume. The integration in eqn. 4 must be performed over a volume enclosing the geometrical defect and large enough to also enclose the mode's electromagnetic energy that spills outside the slab. In

addition, the search for the maximum value of the electrical energy must be carried out in the same volume and preferably along the symmetry planes of the structure. This is to avoid the numerical artefact of high electric field at certain dielectric interfaces due to the discretisation of geometry necessary for the finite difference computation.

With these considerations, the FDTD technique is a flexible tool to calculate resonant frequencies, field and energy distributions of resonant modes, as well as their  $Q$  and effective volume. All this information is necessary for the proper design of an efficient cavity-enhanced light-emitting diode.

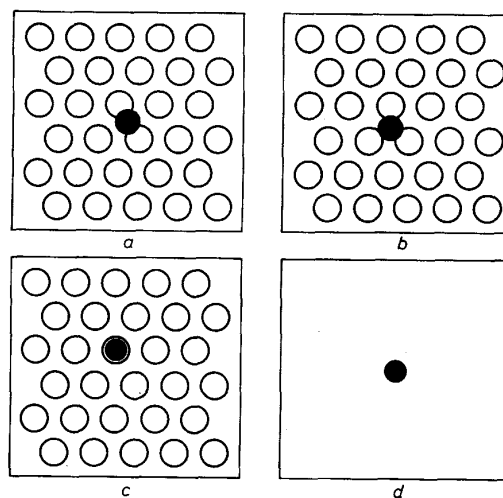


**Fig. 3** Four different cavity configurations in the finite size photonic crystal  
a Defect introduced by adding extra material to the bridge between two holes; b Defect introduced in the spot between three holes; c Defect consists of added material in the centre of a hole; d Dielectric cylinder resting on a glass slab (for comparison)

#### 3.1 Analysed structures

A traditional way of creating a donor defect mode is to fill one hole with semiconductor material. However, there are two other high-symmetry points in the Wigner-Seitz cell in addition to the centre of a hole that may be good locations for a defect. We studied modes created by adding extra material in the middle of the bridge between two holes, in the spot between three holes, and in the centre of a hole, as shown in Fig. 3a, b and c. These Figures show the finite lateral size of the photonic crystal in the actual structures investigated. For comparison, we have also studied the properties of the fundamental mode of a single dielectric cylinder ( $\epsilon = 12$ ) located on the same glass substrate ( $\epsilon = 2.25$ ) supporting the 2-D photonic crystal (Fig. 3d). These structures can be described by three independent dimensionless parameters: normalised thickness  $t/a$ , normalised radius of the holes  $r/a$  and normalised size of the radius defect  $r_d/a$ . Therefore, optimisation of the dimensionless effective volume  $f$  has to be performed in the three-dimensional parameter space:

$$f(t/a, r/a, r_d/a) = \frac{\int \epsilon(\mathbf{r})\mathbf{E}^2(\mathbf{r})d^3\mathbf{r}}{(\lambda/2n)^3 (\epsilon(\mathbf{r})\mathbf{E}^2(\mathbf{r}))_{max}} \quad (5)$$

#### 3.2 Cavity characteristics

Relative thickness  $t/a$  of the structure did not significantly influence the mode volume results. For all the

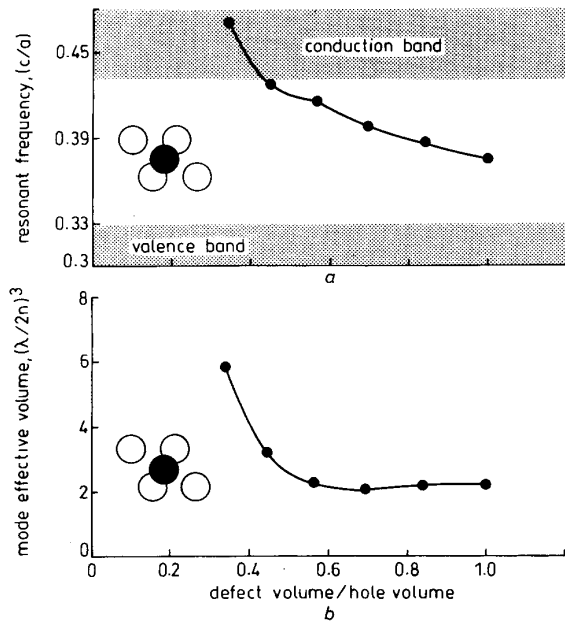


**Fig. 4** Evolution for defect placed on the bridge between two holes  
*a* Resonant frequency of the mode, *b* Effective mode volume in units of  $(\lambda/2n)^3$

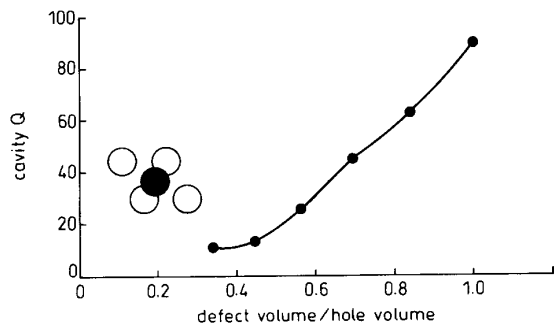


**Fig. 5** Evolution of cavity *Q*-factor for a defect placed on the bridge between two holes

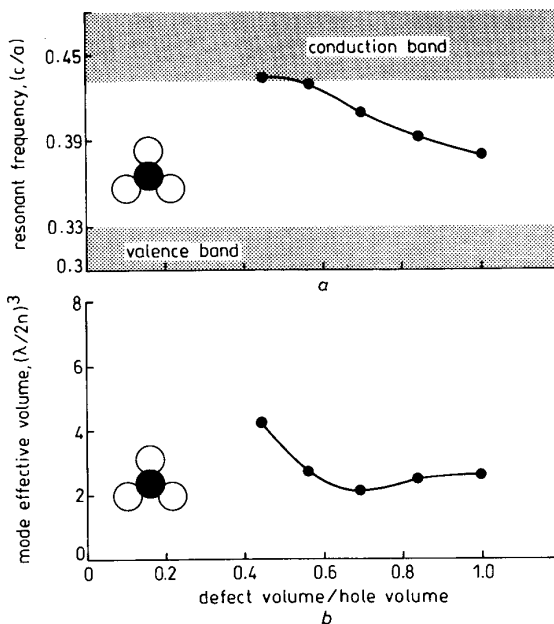


**Fig. 6** Evolution for defect placed in the spot between three holes  
*a* Resonant frequency of the mode, *b* Effective mode volume in units of  $(\lambda/2n)^3$

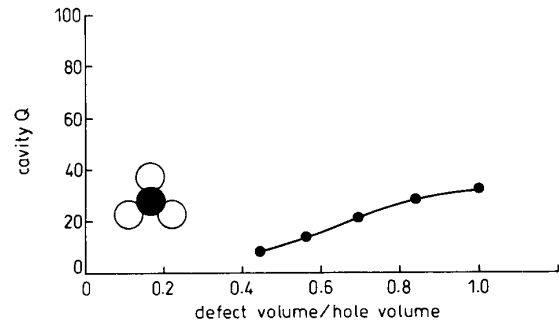


**Fig. 7** Evolution of cavity *Q*-factor for defect placed in the spot between two holes

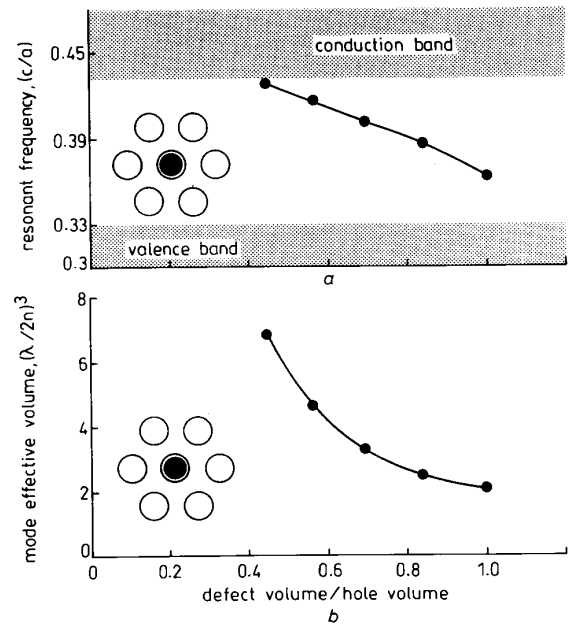


**Fig. 8** Evolution for defect placed on the centre of a hole  
*a* Resonant frequency of the mode, *b* Effective mode volume in units of  $(\lambda/2n)^3$

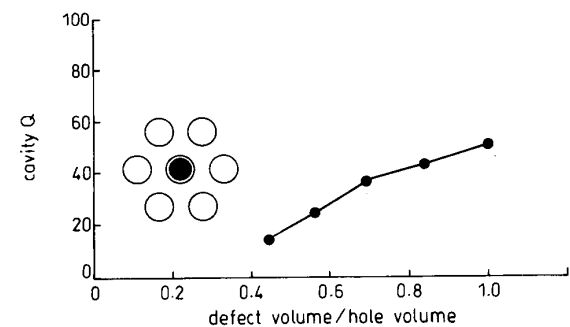


**Fig. 9** Evolution of the cavity *Q*-factor for defect placed at the centre of a hole

studied geometries, the best effective volume was achieved at  $t/a \sim 1/3$ . For technological reasons, the walls between holes should not be too thin. We have chosen  $r/a = 0.4$ , even though larger values of  $r/a$  may produce slightly better results. Figs 4-9 show the variation of frequency, the normalised effective volume, and the *Q* of the lowest order resonant modes against defect size for different cavity geometries. For comparison, we have also studied the resonant modes of a single cylindrical dielectric cavity (Fig. 3*d*). Typically for

all donor modes, the frequency of the mode emerges from the conduction band-edge at  $0.43 c/a$  and decreases towards the frequency  $0.33 c/a$  of the valence band. As can be seen from Figs. 4–9, the resonant frequencies of all structures with the same defect size are roughly the same. This suggests the alternative point of view of the defect mode as the mode of a single cylindrical resonator 'tuned' to the forbidden gap of the photonic crystal to provide additional mode confinement and higher  $Q$ . For small defect size, quality factors are normally on the order of 10. As the mode volume reaches its minimum,  $Q$  goes up to 40 or even up to 90, as in the case of the bridge defects. It is typical for all modes to have cavity  $Q$  increasing as mode volume decreases. Indeed, the more tightly localised the mode is, the smaller its tails outside of a finite sized photonic crystal. By comparison, the cavity  $Q$  of an isolated cylinder [14] is  $0.016 \times n^3 \approx 7$  and mode volume is  $4.52(\lambda/2n)^3$ , under our conditions. Probably the most interesting feature is that the minimum of the effective volumes is about  $V_{eff} \approx 2(\lambda/2n)^3$  for all three defect types. This makes us wonder if there is a fundamental lower limit on the volume size achievable with a certain dielectric material. We believe the mode volume results for 3-D photonic crystal structures with full 3-D confinement would actually be quite similar, since index guiding provides commensurate vertical confinement.

Computation of the flux of the Poynting vector through a surface enclosing the slab reveals that most of the energy of the defect mode leaks in the vertical direction, rather than being guided by the slab. Therefore, increasing the lateral size of the crystal is not likely to significantly increase the cavity  $Q$ . This is an extremely valuable feature in view of possible applications of this type of resonant cavity in light-emitting diodes.

Figs. 10 and 11 show the electric field and energy density distribution of the modes with the smallest effective volumes for all the configurations studied, along a  $z = \text{const}$  plane in the middle of the slab. The electric energy density reaches its maximum almost in the centre of the dielectric slab. Electric energy density is coded with colours in Figs. 10 and 11, and the corresponding projection of the electric field onto the horizontal plane is shown as a vector plot. All these modes are predominantly TE, i.e. the electric field mostly oscillates in the  $xy$  plane. Owing to different locations of the defect, these modes have different symmetries.

Structures with a defect introduced into the bridge between two and three holes have  $C_{2v}$  and  $C_{3v}$  symmetry, respectively, and their resonant modes are not degenerate. These modes bear close resemblance with the 'donut' mode  $TE_{010}$  of a cylindrical cavity, shown in Fig. 11b.

Considering the case of a defect created by adding material to the centre of a hole, the smallest effective mode volume is surprisingly achieved for  $r_d/a = 0.4$ , i.e. when the hole is completely plugged. The electric energy distribution of the resonant mode (Fig. 11a) has a maximum in the centre, which makes the mode a prospective candidate for use in resonant-cavity LED applications, where the active material is placed in the centre of the filled hole. Moreover, since this structure has  $C_{6v}$  symmetry, the resonant mode is doubly degenerate. According to eqn. 1, this fact implies  $g = 2$  in the formula of the enhancement factor. For example, in the

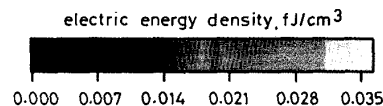
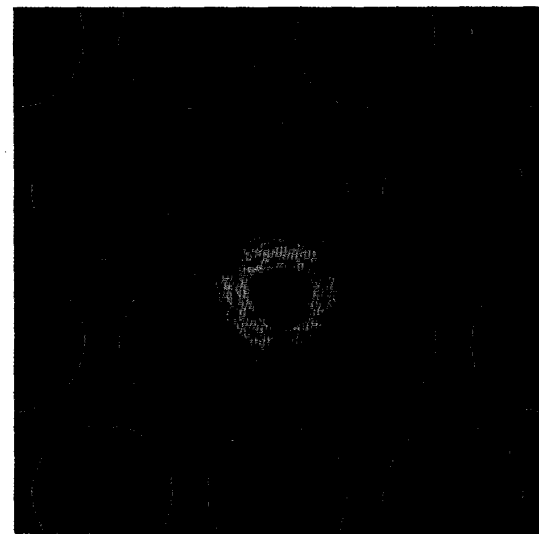


**Fig. 10** Mode pattern, in the plane of the structure, for the modes with the smallest effective mode volumes

Energy density distribution in the  $xy$  plane is coded with colours; in-plane electric field is shown as a vector plot; concentration of electric energy happens in those regions where some material was added

*a* Added material in the bridge between two holes

*b* Added dielectric material in the spot between three holes

semiconductor light emitter  $In_{0.53}Ga_{0.47}As$ , with  $Q_m = 10$  at room temperature, plugging  $V_{eff} = 2(\lambda/2n)^3$  into eqn. 1 gives a five-fold spontaneous emission enhancement  $\Gamma/\Gamma_0 = 5$ .

#### 4 Conclusions

The defect modes in a dielectric slab photonic crystal have been numerically optimised with respect to the mode volume using the finite difference time domain algorithm. A record low value of only  $2(\lambda/2n)^3$  is shown to be achievable in three different configurations. This small mode volume can lead to a significant enhance-

ment of spontaneous emission rates in semiconductor nano-cavities due to the Purcell effect.

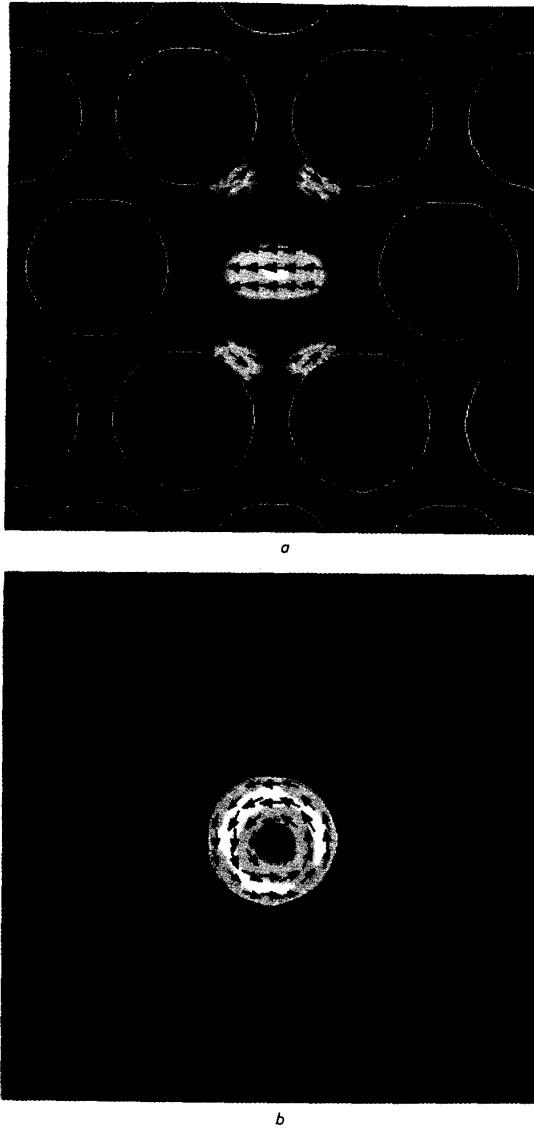


**Fig. 11** Mode pattern, in the plane of the structure, for the modes with the smallest effective mode volumes  
Energy density distribution in the  $xy$  plane is coded with colours; in-plane electric field is shown as a vector plot; concentration of electric energy happens in those regions where some material was added  
*a* Hole plugged up with dielectric material, *b* Single dielectric cylinder on a glass substrate; cavity  $Q \sim 7$  and the effective mode volume  $\sim 4.5(\lambda/2n)^3$  for cylinder with same dimensions as in Fig. 10*a* and *b*

## 5 Acknowledgments

This work was supported by US Army MURI under contract DAAH04-96-1-0389.

## 6 References

- 1 YABLONOVITCH, E.: 'Inhibited spontaneous emission in solid-state physics and electronics', *Phys. Rev. Lett.*, 1987, **58**, (20), pp. 2059–2062
- 2 PURCELL, E.M.: 'Spontaneous emission probabilities at radio frequencies', *Phys. Rev.*, 1946, **69**, pp. 681–686
- 3 BORODITSKY, M., COCCIOLI, R., and YABLONOVITCH, E.: 'Analysis of photonic crystals for light emitting diodes using the finite difference time domain technique'. Photonics West 1998, San Jose, CA, 28–29 January 1998

- 4 GÉRARD, J., SERMAGE, B., GAYRAL, B., LEGRAND, B., COSTARD, E., and TIERRY-MIEG, V.: 'Enhanced spontaneous emission by quantum boxes in a monolithic optical microcavity', *Phys. Rev. Lett.*, 1998, **91**, (5), pp. 1110–1113
- 5 SCHUBERT, F., WANG, Y.-H., CHO, A.Y., TU, L.-W., and ZYDZIK, G.J.: 'Resonant cavity light-emitting diode', *Appl. Phys. Lett.*, 1992, **60**, (8), pp. 921–923
- 6 DE NEVE, H., BLONDELLE, J., BAETS, R., DEMEESTER, P., VAN DAELE, P., and BORGHS, G.: 'High efficiency planar microcavity LEDs: comparison of design and experiment', *IEEE Technol. Lett.*, 1995, **7**, (287)
- 7 FORESI, J., VILLENEUVE, P.R., FERRERA, J., THOEN, E.R., STEINMEYER, G., FAN, S., JOANNOPOULOS, J.D., KIMERLING, L.C., SMITH, H.I., and IPPEN, E.P.: 'Photonic-bandgap microcavities in optical waveguides', *Nature*, 1997, **390**, (6656), pp. 143–145
- 8 SAKODA, K.: 'Numerical study on localized defect modes in two-dimensional triangular photonic crystals', *J. Appl. Phys.*, 1998, **84**, (3), pp. 1210–1214
- 9 MUR, G.: 'Absorbing boundary conditions for the finite-difference approximation of the time-domain electromagnetic-field equations', *IEEE Trans. Electromagn. Comput.*, 1981, **23**, (4), pp. 377–382
- 10 GEDNEY, S.: 'An anisotropic perfectly matched layer-absorbing medium for the truncation of FDTD-lattices', *IEEE Trans. Antennas Propag.*, 1996, **44**, (12), pp. 1630–1639
- 11 BERENGER, J.-P.: 'A perfectly matched layer for the absorption of electromagnetic waves', *J. Comput. Phys.*, 1994, **114**, (2), pp. 185–200
- 12 FAN, S., VILLENEUVE, P.R., JOANNOPOULOS, J.D., and SCHUBERT, E.F.: 'High extraction efficiency of spontaneous emission from slabs of photonic crystals', *Phys. Rev. Lett.*, 1997, **78**, pp. 3294–3297
- 13 BORODITSKY, M., and YABLONOVITCH, E.: 'Photonic crystals boost light emission', *Physics World*, 1997, **7**, pp. 53–54
- 14 DE SMEDT, R.: 'Correction due to a finite permittivity for a ring resonator in free space', *IEEE Trans.*, 1984, **MTT-32**, (10), pp. 1288–1293
- 15 MILONNI, P.: 'The quantum vacuum: an introduction to quantum electrodynamics' (Academic Press, Boston, 1994)

## 7 Appendix: Enhancement of spontaneous emission in semiconductor nano-cavities

The Purcell enhancement factor [2] should be modified when considering the generation of light in semiconductor quantum well (QW) structures. The classical electric field of the cavity mode  $\mathbf{E}(\mathbf{r})$  has to be normalised  $\mathbf{E} \rightarrow \alpha\mathbf{E}$  so that

$$\frac{1}{4\pi} \int \varepsilon(\mathbf{r})(\alpha\mathbf{E}(\mathbf{r}))^2 d^3\mathbf{r} = \frac{\hbar\omega_0}{2} \quad (6)$$

where  $\varepsilon$  is the material dielectric constant and  $\omega_0$  is the resonant frequency of the cavity. This gives the normalisation factor

$$\alpha^2 = \frac{2\pi\hbar\omega_0}{\int \varepsilon(\mathbf{r})\mathbf{E}^2(\mathbf{r})d^3\mathbf{r}} \quad (7)$$

In the above equations, the integration extends over the quantisation volume. Spontaneous emission rate at frequency  $\omega$  into the resonant mode  $\omega_0$  at a given point  $\mathbf{r}$  follows from the Fermi golden rule and equals

$$\Gamma(\mathbf{r}) = \frac{2\pi}{\hbar} \langle (\mathbf{d} \cdot \alpha\mathbf{E}(\mathbf{r})) \rangle^2 \frac{\Delta\omega g}{2\pi\hbar((\omega - \omega_0)^2 + (\Delta\omega/2)^2)} \quad (8)$$

where  $\mathbf{d}$  denotes the atomic moment dipole,  $\Delta\omega$  is the cavity line width, and  $g$  is the degeneracy of the cavity mode.

The last term in eqn. 8 represents the Lorentzian density of electromagnetic modes; there are  $g$  modes in the frequency range  $\Delta\omega$ . The dot product  $(\mathbf{d} \cdot \alpha\mathbf{E}(\mathbf{r}))$  has to be averaged over the possible orientations of the atomic dipole moment. At this point, we need to take the specific of optical transition in semiconductor quantum wells. First, electron-heavy hole transitions are the major contributor to the spontaneous emission. Secondly, these transitions are only allowed if the

dipole moment of the transition lies in the plane of the quantum well, so that  $d_x^2 = d_y^2 = d^2/2$ ,  $d_z^2 = 0$ . If the mode's electric field is also in the QW plane, as happens for TE modes, then the average  $\langle (\mathbf{d} \cdot \alpha \mathbf{E}(\mathbf{r})) \rangle^2 = (1/2)d^2(\alpha \mathbf{E}(\mathbf{r}))^2$ . Note that, in the case of bulk semiconductor, or for interaction with random modes, the above prefactor would have been 1/3.

If the active material is placed in the point of maximum electric field of the mode, the emission rate is

$$\Gamma = \frac{2\pi}{\hbar} \frac{d^2}{2} (\alpha \mathbf{E}_{max})^2 \frac{\Delta\omega g}{2\pi\hbar((\omega - \omega_0)^2 + (\Delta\omega/2)^2)} \quad (9)$$

If the line width of the cavity  $\Delta\omega$  is much smaller than emission spectrum width of the active material  $\Delta\omega_m$ , integration over the frequencies leads to

$$\Gamma = \frac{2\pi}{\hbar} \frac{d^2}{2} (\alpha \mathbf{E}_{max})^2 \frac{g}{\hbar\Delta\omega_m} \quad (10)$$

Introducing the value of the normalisation factor  $\alpha^2$  gives

$$\Gamma = \frac{\omega_0}{\Delta\omega_m} \frac{2g\pi^2 d^2}{\hbar} \frac{\mathbf{E}_{max}^2}{\int \varepsilon(\mathbf{r}) \mathbf{E}^2(\mathbf{r}) d^3\mathbf{r}} \quad (11)$$

Spontaneous emission rate in the bulk can be calculated using the classical formula [15]:

$$\Gamma_0 = \frac{4n d^2 \omega^3}{3\hbar c^3} = \frac{4n d^2 8\pi^3}{3\hbar \lambda^3} \quad (12)$$

Thus, overall enhancement factor, which can be used as a figure of merit for optimisation of a resonant-cavity structure, becomes

$$\frac{\Gamma}{\Gamma_0} = Q_m g \frac{3\lambda^3}{16\pi n} \frac{\mathbf{E}_{max}^2}{\int \varepsilon(\mathbf{r}) \mathbf{E}^2(\mathbf{r}) d^3\mathbf{r}} \quad (13)$$

where  $Q_m = \omega_0/\Delta\omega_m$  is the quality factor of the material. Introducing the mode volume  $V_{eff}$

$$V_{eff} = \frac{\int \varepsilon(\mathbf{r}) \mathbf{E}^2(\mathbf{r}) d^3\mathbf{r}}{(\varepsilon(\mathbf{r}) \mathbf{E}^2(\mathbf{r}))_{max}} \quad (14)$$

the enhancement of spontaneous emission rate can be recast in the following form:

$$\frac{\Gamma}{\Gamma_0} = \frac{3Q_m g (\lambda/2n)^3}{2\pi V_{eff}} \quad (15)$$

This expression differs from that originally derived by Purcell by a degeneracy factor  $g$  and a factor of  $\pi/4$ , which follows from Lorentzian normalisation and the polarisation averaging in quantum well structures.